CFD Letters

Journal homepage:
https://semarakilmu.com.my/journals/index.php/CFD_Letters/index
ISSN: 2180-1363

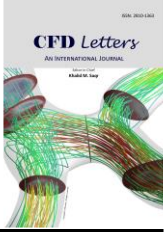


# Moving Mesh as Transient Approach for Pico Scale Undershot Waterwheel

Imam Syofii[1], Dewi Puspita Sari[1,*], Dendy Adanta[2], Muhammad Amsal Ade Saputra[2], Wadirin[2]

[1] Study Program of Mechanical Engineering Education, Faculty of Teacher Training and Education, Universitas Sriwijaya, Indralaya 30662, South Sumatera, Indonesia
[2] Department of Mechanical Engineering, Faculty of Engineering, Universitas Sriwijaya, Indralaya 30662, South Sumatera, Indonesia

**ARTICLE INFO**

***Article history:***
Received 13 June 2022
Received in revised form 8 July 2022
Accepted 23 July 2022
Available online 31 August 2022

***Keywords:***
Moving Mesh; Transient Approach; Undershot Waterwheel; Pico hydro

**ABSTRACT**

The computational fluid dynamics (CFD) method is often used for undershot waterwheel (USWW) studies. The CFD method is a suitable solution for investigating physical flow phenomena on USWW so that its energy conversion process can be appropriately understood. The transient simulation is necessary to study the flow of physical phenomena. However, there is no recommendation for the transient approach for USWW. The boundary conditions for the transient approach often used for rotating case objects is a moving mesh. Therefore, this study investigates moving mesh as a USSW transient approach to predict its performance. Based on the results, the average deviation from simulation results to experimental data of torque is 22.1%, mechanical power is 5.75%, and efficiency is 5.75%. The average deviation reading of torque is 2.93 N·m (not a significant difference), mechanical power is 0.47 W, and efficiency is 1.19%. Further, the curve data simulation results to experimental data show a similar pattern, expressed by exponential for torque and polynomial for mechanical power and efficiency. Thus, a transient approach using the moving mesh feature is recommended for the USWW case; because the data pattern and reading deviation are reasonable.

## 1. Introduction

In Indonesia, the need for electrical energy increases every year. Natural resources that cannot be renewed are limited, so the use of renewable energy continues to be developed as an energy source for power generation. There are limited non-renewable fuels, so renewable energy continues to be developed as a source of energy for generating electricity [1]. Therefore, water energy is prospective to be used as an energy supply for power plants [2,3].

The undershot waterwheel (USWW) is a type of turbine often used in a power plant [4]. The USWW has the advantages of a relatively simple design, simple maintenance, and relatively low repair costs [5]. The USWW can operate in the discharge of 0.9 to 1.2 $m^3/s$ and head in the condition of under-very-low-head or 0.1to 1.5 m [6,7].

The issue of global warming makes the feasibility study of the USWW as a power plant continue to be developed [8,9]. Sari *et al.,* [4] studied the best ratio of the wheel tangential velocity to

* *Corresponding author.*
*E-mail address: dewipuspita@fkip.unsri.ac.id (Dewi Puspita Sari)*

https://doi.org/10.37934/cfdl.14.8.3342

upstream water velocity ($U/C_1$) for USWW design. Based on the results, 0.4 $U/C_1$ indicates a good agreement for USWW design [2]; this hypothesis is based on the experimental data, where the condition is not similar to Denny's [10] mathematical analysis. Nishi *et al.,* [11] adopt the shape of a crossflow turbine blade (curvature) to be applied to the USWW. Based on the results, the USWW blade shape influences mechanical power ($P_{mech}$), where the straight shape is preferred over curvature [11]. Then, the ratio of blade height to submerge ($h/h_{up}$) becomes an important concern. Yah *et al.,* [12] investigated that 1 $h/h_{up}$ is the ideal condition to reach the optimum USWW performance. Since the results by Yah *et al.,* [12] are not comprehensive, Warjito *et al.,* [6] re-investigate the $h/h_{up}$ ratio using the computational fluid dynamics (CFD) method. Based on hypotheses Yah *et al.,* [12] and Warjito *et al.,* [6], the 1 $h/h_{up}$ is considered realistic to be applied in USWW for the run of river conditions. Then, Warjito *et al.,* [13] adopted the Pelton turbine blade number (z) equation for the USWW by computational fluid dynamics (CFD) method. Warjito *et al.,* [13] used the boundary condition is 1 $h/h_{up}$, adaptation of the z equation for USWW yields 8, hence it is considered unreasonable for larger scales.

Furthermore, Adanta *et al.,* [14] evaluate the proposed equation z by Warjito *et al.,* [13]. Evaluation using the CFD method with a six-degrees of freedom (6-DoF) feature accommodates the moment of inertia of each wheel [14]. Based on the results, the highest performance is produced by 20 blades; however, more stable performance is produced by 8 blades [14]. A provisional hypothesis is determining the z USWW cannot yet be proposed. USWW's hydraulic behaviour still needs to be studied more using the CFD method. The CFD method can visualise the flow field in more detail than experimental and analytical [15]. The transient approach using 6-DoF is considered inefficient for case USWW because it requires a large computational power (long time) due to long stable torque conditions [15]. A moving mesh is a transient approach that is appropriate and requires lower computational power. Therefore, this study aims to examine the reliability of the moving mesh approach for USWW transient conditions to investigate its hydraulic behaviour.

## 2. Methodology

### *2.1 Computational Method*

ANSYS® FLUENT 18.1™ Academic version was used as the computational software. The two-dimensional (2D) analysis approach represents real conditions for a case undershot waterwheel [5]. Undershot waterwheel simulation does not involve heat; hence the mass conservation approach is applied. The mass conservation equation in the transient condition is [16]:

$$\frac{\partial \ \rho}{\partial t}+\frac{\partial \ \rho u_j}{\partial x_j}=0 \tag{1}$$

Then, the flow that occurs is assumed to be turbulence. The turbulent flow approach based on Reynolds Average Navier-Stokes (RANS) is considered capable for the undershot waterwheel simulation [17,18]. The equation of the RANS approach is [19,20]:

$$\frac{\partial \ \rho u_i}{\partial t}+\frac{\partial \ \rho u_i u_j}{\partial x_j}=-\frac{\partial p}{\partial x_i}+\frac{\partial \ \tau_{ij}-\rho u_i{}' u_j{}'}{\partial x_j}+\rho g_i \tag{2}$$

Where p is pressure, $\tau_{ij}$ is shear stress, and $-\rho u_i'u_j'$ is Reynolds stress. For the $-\rho u_i'u_j'$ is [21]:

$$-\rho u_i' u_j' = \mu_t \left( \frac{\partial u_i}{\partial x_j} + \frac{\partial u_j}{\partial x_i} \right) - \frac{2}{3} \left( \rho k + \mu_t \frac{\partial u_i}{\partial x_i} \right) \delta_{ij} \tag{3}$$

The Reynolds stress has two variable unknowns: turbulence kinetic energy (*k*) and viscous stress ($\mu_t$) [22]. This study applied the k-ε turbulence model to predict the fluid's kinetic energy (k) and turbulence dissipation rate (ε). The standard k−ε turbulence model equation is for k [22,23]:

$$\frac{\partial \rho k}{\partial t} + \frac{\partial \rho k u_i}{\partial x_j} = \frac{\partial}{\partial x_i} \left( \left( \mu + \frac{\mu_t}{\sigma_k} \right) \frac{\partial k}{\partial x_j} \right) + G_k + G_b + \rho \varepsilon + Y_M + S_k \tag{4}$$

And for ε [22]:

$$\frac{\partial \rho \varepsilon}{\partial t} + \frac{\partial \rho \varepsilon u_i}{\partial x_j} = \frac{\partial}{\partial x_i} \left( \left( \mu + \frac{\mu_t}{\sigma_\varepsilon} \right) \frac{\partial \varepsilon}{\partial x_j} \right) + C_{1\varepsilon} \frac{\varepsilon}{k} G_k + C_{3\varepsilon} G_b - C_{2\varepsilon} \rho \frac{\varepsilon^2}{k} + S_\varepsilon \tag{5}$$

The VoF is a numerical approach to predicting the interaction of two or more fluids, such as water and air. At the inlet, no accompanying air (100% inlet is water); the setting VoF of water ($\alpha_w$) value was 1, and the VoF of air ($\alpha_a$) was 0. At the outlet, the air is the dominant fluid; the $\alpha_a$ of 1. Numerical calculation of the nature of the mixture of density (ρ) [22]:

$$\rho = \alpha_w \rho_w + \alpha_a \rho_a \tag{6}$$

and viscosity (μ) [22]:

$$\mu = \alpha_w \mu_w + \alpha_a \mu_a \tag{7}$$

Figure 1 shows the boundary conditions used: inlet (velocity inlet), outlet (pressure outlet), stator (interface domain irrigation), and rotor (interface domain wheel). The velocity inlet is 1 m/s, and the pressure outlet is 0 Pa (atmospheric pressure). There are five variations of the wheel rotation (n): 0 rpm 5 rpm, 10 rpm, 15 rpm, and 20 rpm; the n adjusts to the experimental data [5].

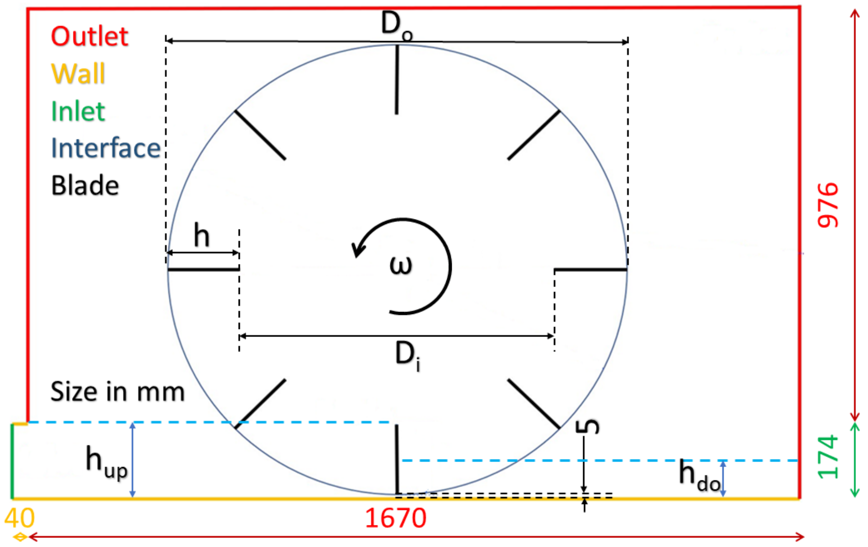

**Fig. 1.** Boundary condition CFD method

## *2.2 Mechanical Power and Performance Analysis*

The τ is the main parameter or data of the computational results, while the n is the boundary condition. The $P_{mech}$ is the function of the τ and n, which become:

$$P_{mech} = \tau \cdot \omega \tag{8}$$

Performance or efficiency (η) is the ratio of $P_{mech}$ to the potential energy of water ($P_{pot}$). $P_{pot}$ is a function of fluid density (ρ), discharge (Q), head (h), and gravity (g). The analysis of the η is:

$$\eta = \frac{P_{mech}}{P_{pot}} \tag{9}$$

## *2.3 Independence Test Method*

Torque (τ) is the parameter used for the mesh independency test. Grid convergency index (GCI) analysis is used to mesh the independency test. The GCI is capable of establishing each mesh number error to the exact value ($\tau_{x \to \sim}$). The GCI calculation analysis is:

$$GCI_{fm} = F_s \left| \frac{1}{\tau_{fine}} \frac{\tau_{medium} - \tau_{fine}}{r_{fm}^{q_n} - 1} \right| \cdot 100\% \tag{10}$$

$F_s$ is a safety factor of 1.25, *r* is the grid refinement ratio ($r_{fm}=(M_{fine}/M_{medium})^{0.5}$), and q is the order of convergence observed. M is mesh number. The normalisation of mesh number (h) is done by inverse comparison, where $h_{fi}$ is $1_c$, $h_f$ is $h_{fi} \cdot r_{ff}$, $h_m$ is $h_f \cdot r_{fm}$, and $h_c$ is $h_m \cdot r_{mc}$.

$$q_{n+1} = \ln \left| \left( \frac{\tau_{coarse} - \tau_{medium}}{\tau_{medium} - \tau_{fine}} \left( r_{fm}^{q_n - 1} \right) \right) + r_{fm}^{q_n} \right| / \ln \left( r_{fm} \cdot r_{mc} \right) \tag{11}$$

Further, the extrapolation approach was used to predict the $\tau_{x\to\sim}$ [24]. The prediction by applying the two finest resolutions; the concept extrapolation calculation is [24]:

$$\tau_{x\to\sim} = \tau_{fine} - \left( \frac{\tau_{medium} - \tau_{fine}}{r_{fm}^{\,q_n+1} - 1} \right) \quad (12)$$

The Courant number (Cn) analysis is used for timestep independency analysis to determine the timestep size (Δt). The $C_n$ is the ratio of fluid velocity to Δt per Δx, becoming:

$$C_n = u_i \cdot \frac{\Delta t}{\Delta x} \quad (13)$$

The $C_n$ is a non-dimensional analysis representing the time a fluid particle stays in one mesh cell [22]. The $C_n$ is ideally below 1 ($C_n < 1$); since it exceeds 1 like a particle skips the cell, the timestep is higher than mesh size [22].

## 3. Results and Discussion

### *3.1 Mesh independency Test Results*

Four mesh numbers are compared to get the optimum mesh number: 21.3k (coarse), 33.4k (medium), 50.5k (fine), and 85.1k (finest). From the mesh number, the $r_{ff}$ is 1.3, the $r_{fm}$ is 1.23, and the $r_{mc}$ is 1.25; then the $h_{fi}$ of 1, $h_f$ of 1.3, $h_m$ of 1.6, and $h_c$ of 2. The τ of each mesh is 15.2 N·m (coarse), 35.9 N·m (medium), 36.1 N·m (fine), and 36.2 N·m (finest). Then, determine q using Eq. (9):

$$q_{n+1} = \ln\left| \left( \frac{35.9 - 36.1}{36.1 - 36.2} \left( 1.3^{4.03-1} \right) \right) + 1.3^{4.03} \right| / \ln\left( 1.3 \cdot 1.23 \right) = 4.03$$

Then, extrapolation of $\tau_{x\to\sim}$ using Eq. (10):

$$\tau_{x\to\sim} = 36.2 - \left( \frac{36.1 - 36.2}{1.3^{4.03+1} - 1} \right) = 36.25$$

Finally, calculate GCI using Eq. (7). Example GCI calculation for case fine to finest mesh is:

$$GCI_{ff} = 1.25 \left| \frac{1}{36.2} \frac{36.1 - 36.2}{1.3^{4.03} - 1} \right| \cdot 100\% = 0.19\%$$

Figure 2 shows the results of the GCI calculation. From Figure 2, $GCI_{ff}$ has an error of 0.19%, $GCI_{fm}$ of 0.53%, and $GCI_{mc}$ of 48.9%. Based on Figure 2, 50.5k (fine) mesh is used for this case because it has an error below 1% (range from 0.19% to 0.53%). Figure 3 is the visualisation of 50.5k mesh.

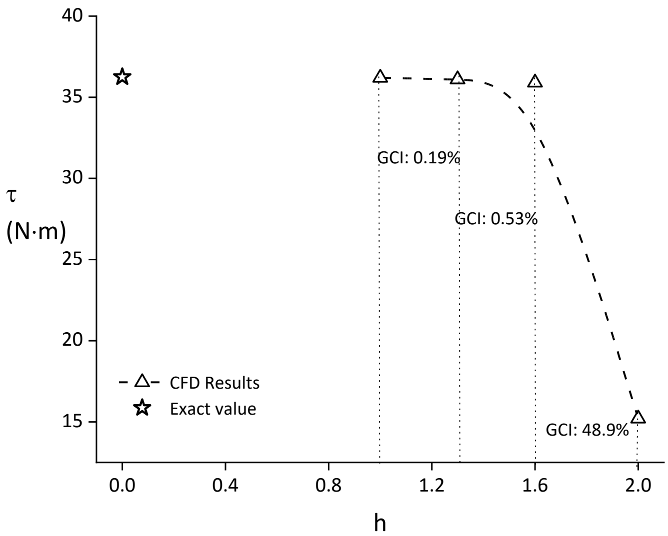


**Fig. 2.** GCI results

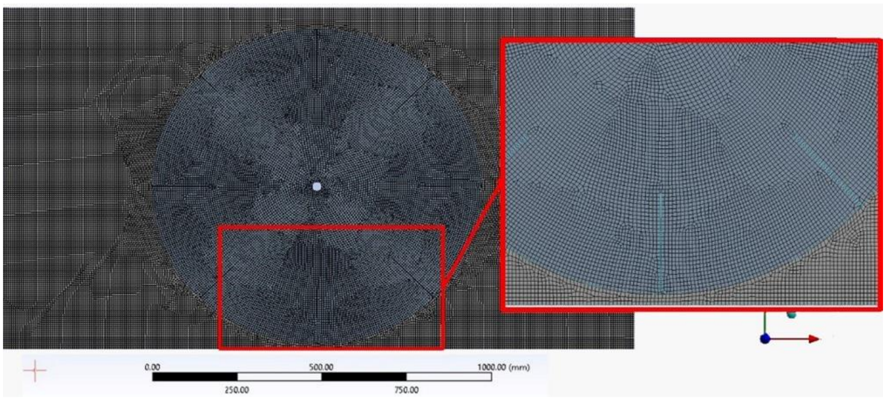

**Fig. 3.** Visualisation of 50.5k mesh USWW

### *3.2 Timestep Independency Test Results*

Three timestep size are compared to get the its optimum: 0.0016s (625 Hz), 0.001s (1000 Hz), and 0.0005s (2000 Hz). The 50.5k mesh number has an average size of 0.001736 m. Further, the average local water (fluid) velocity at 0.1 m from the inlet and 0.1 m from the irrigation wall is 1.09 m/s. Then, calculate the $C_n$ using Eq. (13). Example calculation of the $C_n$ is:

$$C_n = 1.09 \cdot \frac{0.0016}{0.001736} = 1.005$$

Table 1 is the result of the calculation of the $C_n$ for the three timestep sizes. Based on Table 1, the timestep size of 0.001s (1000 Hz) is suitable for this case because of the $C_n$ of below 0.7.

**Table 1**
$C_n$ calculation results

| Δx (m) | Timestep size (s) | Frequency (Hz) | Average local fluid velocity (m/s) | $C_n$ |
|---|---|---|---|---|
| 0.001736 | 0.0016 | 625 | 1.09 | 1.005 |
| | 0.001 | 1000 | | 0.628 |
| | 0.0005 | 2000 | | 0.314 |

### *3.3 Results*

Based on Figure 4, the average deviation of τ simulation results in experimental data of 22.1%. The deviation in percentage is categorised as significant; however, the average reading is 2.93 N·m; not a significant difference. Then, the τ curve by simulation results to experimental data shows a similar pattern. Figure 4 indicates that the simulation data is verified. Furthermore, the average deviation of $P_{mech}$ of simulation results to the experimental data is 5.75%, and the reading categorised of 1.89 W. Deviation $P_{mech}$ and τ is similar because $P_{mech}$ is the function of τ and the relation is proportional (Eq. (8)).

Based on simulation results and experimental data, USWW has a peak operation at 10 rpm. From Figure 4, the USWW operating range for this case is recommended from 5 rpm to 15 rpm.

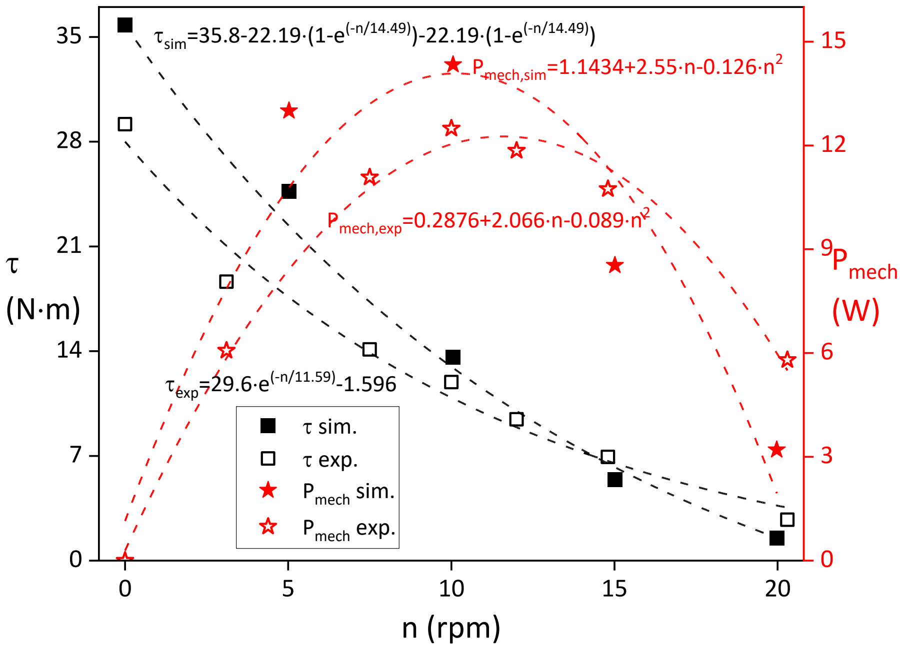


**Fig. 4.** Relation of τ and $P_{mech}$ to n

Figure 5 shows the relation of η to n by simulation results and experimental data. The relation of η to n is a polynomial quadratic; the peak operation at 10 rpm with η is 35.83% from simulation results and 31.22% from experimental data.

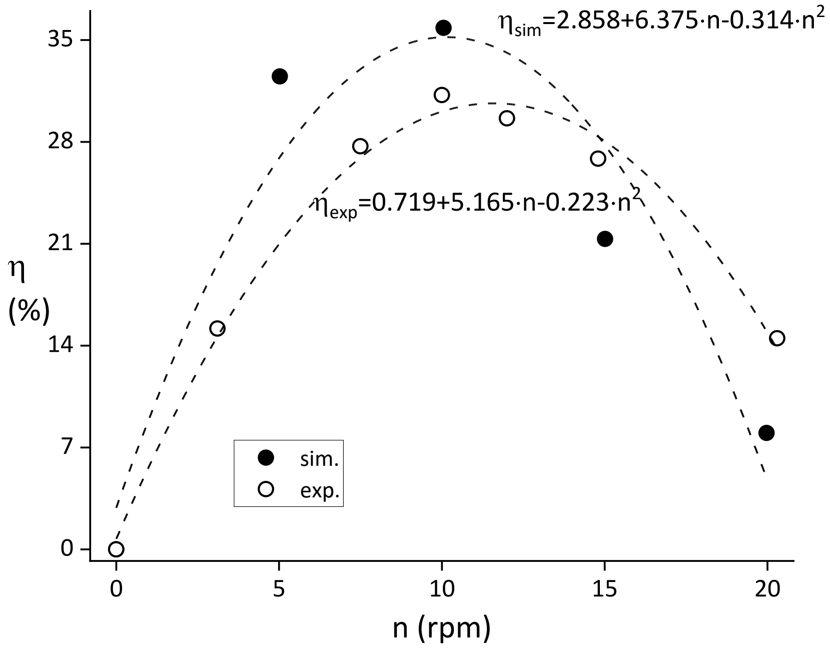


**Fig. 5.** Relation of η to n

Figure 4 and Figure 5 confirm that experimental data confirms the simulation results are valid and verified. Hence, a transient approach using the moving mesh feature is recommended for the USWW case; because the data pattern and reading deviation are reasonable.

*3.4 Discussion*

Figure 6 is the visualisation of water volume fraction by simulation results. Based on Figure 6, there is one active blade, where it can be seen that there is a difference in water levels upstream and downstream. Figure 6 shows that the mechanism of water energy absorbed by the USWW blade is dominated by hydrodynamics force; this hypothesis is similar to Warjito *et al.,* [13].

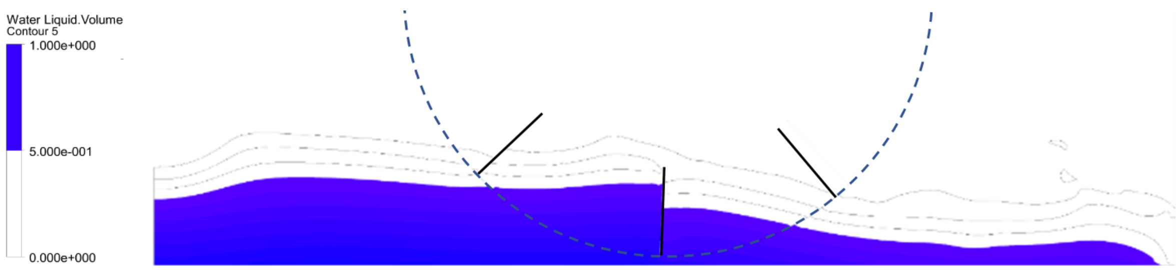


**Fig. 6.** Visualisation of water volume fraction from the simulation result

The absorption of the hydrodynamics force is confirmed in Figure 7. The pressure received by the active blade from top to bottom has increased, and the received force has similar distribution because the relation pressure to force is proportional [25]. The top of the active blade receives less force than the bottom due to the influence of atmospheric pressure [25]. The increases in USWW performance are by increasing the water level gradient upstream to downstream. Furthermore, the visualisation of water volume fraction in Figure 6 is similar to real conditions [5], and the visualisation of pressure distribution in Figure 7 to the analytical method [13].

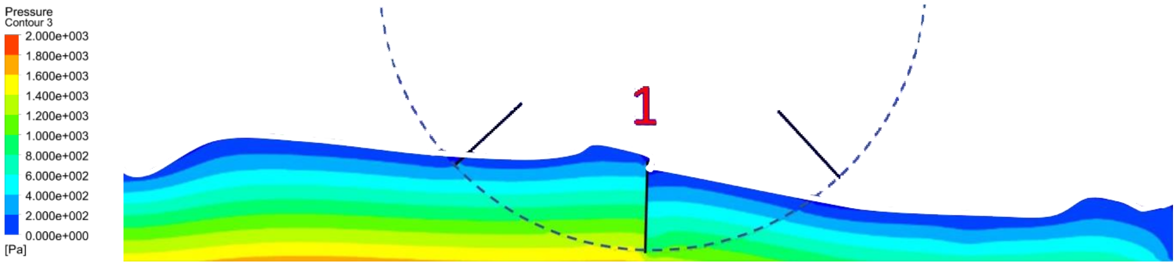


**Fig. 7.** Visualisation of pressure contour by simulation results

## 4. Conclusions

The issue of global warming makes research on renewable energy-based power plants the main focus, and water turbines are no exception. USWW is a water turbine considered appropriate for electrification in remote or rural areas, especially in Indonesia. Using the CFD method in the USWW study is a suitable solution for investigating physical flow phenomena so that the energy conversion process can be appropriately understood. In the CFD method, the boundary conditions for the transient approach often used for rotating case objects is a moving mesh. Therefore, this study investigates moving mesh as a USSW transient approach to predict its performance. Based on the results, the average deviation of $\tau$ from simulation results to experimental data of 22.1%, and $P_{mech}$ and $\eta$ of 5.75%. The average deviation of $\tau$ is categorised as significant; however, the average reading is 2.93 N·m (not a significant difference), and 0.47 W and 1.19% for $P_{mech}$ and $\eta$, respectively. Then, the $\tau$, $P_{mech}$, and $\eta$ curve by simulation results to experimental data shows a similar pattern. Thus, the simulation results are valid and verified by experimental data. Hence, a transient approach using the moving mesh feature is recommended for the USWW case; because the data pattern and reading deviation are reasonable.

## Acknowledgement

This research/publication of this article was funded by DIPA of Public Service Agency of Universitas Sriwijaya 2022. SP DIPA-023.17.2.677515/2022, on December 13, 2021. In accordance with the Rector's Decree Number: 0110/UN9.3.1/SK/2022, on April 28, 2022.

## References

[1] Cifuentes, Oscar Darío Monsalve, Jonathan Graciano Uribe, and Diego Andrés Hincapié Zuluaga. "Numerical Simulation of a Propeller-Type Turbine for In-Pipe Installation." *Journal of Advanced Research in Fluid Mechanics and Thermal Sciences* 83, no. 1 (2021): 1-16. https://doi.org/10.37934/arfmts.83.1.116

[2] Sritram, Piyawat, and Ratchaphon Suntivarakorn. "Comparative study of small hydropower turbine efficiency at low head water." *Energy Procedia* 138 (2017): 646-650. https://doi.org/10.1016/j.egypro.2017.10.181

[3] Darsono, Febri Budi, Rahmad Doni Widodo, Rusiyanto Rusiyanto, and Akhmad Nurdin. "Analysis Of the Effect of Flow Rate and Speed on Four Blade Tubular Water Bulb-Turbine Efficiency Using Numerical Flow Simulation." *Journal of Advanced Research in Fluid Mechanics and Thermal Sciences* 90, no. 2 (2021): 1-8. https://doi.org/10.37934/arfmts.90.2.18

[4] Sari, Dewi Puspita, Helmizar Helmizar, Imam Syofii, Darlius Darlius, and Dendy Adanta. "The effect of the ratio of wheel tangential velocity and upstream water velocity on the performance of undershot waterwheels." *Journal of Advanced Research in Fluid Mechanics and Thermal Sciences* 65, no. 2 (2020): 170-177.

[5] Sari, Dewi Puspita, Imam Syofii, Dendy Adanta, Anthony Costa, Muhammad Agil Fadhel Kurnianto, Sanjaya Nasution, Aji Putro Prakoso, and Fajar Sungging Rahmatullah. "Performance of undershot waterwheel in pico scale with difference in the blades number." *Journal of the Brazilian Society of Mechanical Sciences and Engineering* 44, no. 3 (2022): 1-10. https://doi.org/10.1007/s40430-022-03430-0

[6] Warjito, Warjito, Dendy Adanta, Budiarso Budiarso, Sanjaya B. S. Nasution, and Muhamad Agil Fadhel Kurnianto. "The effect of blade height and inlet height in a straight-blade undershot waterwheel turbine by computational method." *CFD Letters* 11, no. 12 (2019): 66-73.

[7] Quaranta, Emanuele, and Gerald Müller. "Optimization of undershot water wheels in very low and variable flow rate applications." *Journal of Hydraulic Research* 58, no. 5 (2020): 845-849. https://doi.org/10.1080/00221686.2019.1671508
[8] Basar, Mohd Farriz, Nurul Ashikin M. Rais, Azhan Ab Rahman, Wan Azani Mustafa, Kamaruzzaman Sopian, and Kaifui V. Wong. "Optimization of Reaction Typed Water Turbine in Very Low Head Water Resources for Pico Hydro." *Journal of Advanced Research in Fluid Mechanics and Thermal Sciences* 90, no. 1 (2022): 23-39. https://doi.org/10.37934/arfmts.90.1.2339
[9] Khattak, M. A., N. S. Mohd Ali, N. H. Zainal Abidin, N. S. Azhar, and M. H. Omar. "Common Type of Turbines in Power Plant: A Review." *Journal of Advanced Research in Applied Sciences and Engineering Technology* 3, no. 1 (2016): 77-100.
[10] Denny, Mark. "The efficiency of overshot and undershot waterwheels." *European Journal of Physics* 25, no. 2 (2003): 193. https://doi.org/10.1088/0143-0807/25/2/006
[11] Nishi, Yasuyuki, Terumi Inagaki, Yanrong Li, Ryota Omiya, and Junichiro Fukutomi. "Study on an undershot cross-flow water turbine." *Journal of Thermal Science* 23, no. 3 (2014): 239-245. https://doi.org/10.1007/s11630-014-0701-y
[12] Yah, Nor Fadilah, Mat Sahat Idris, and Ahmed Nurye Oumer. "Numerical investigation on effect of immersed blade depth on the performance of undershot water turbines." In *MATEC Web of Conferences*, vol. 74, p. 00035. EDP Sciences, 2016. https://doi.org/10.1051/matecconf/20167400035
[13] Warjito, Warjito, Dendy Adanta, Satrio Adi Arifianto, Sanjaya B. S. Nasution, and Budiarso Budiarso. "Effect of blades number on undershot waterwheel performance with variable inlet velocity." In *2018 4th International Conference on Science and Technology (ICST)*, pp. 1-6. IEEE, 2018.
[14] Adanta, Dendy, Muhamad Agil Fadhel Kurnianto, and Sanjaya BS Nasution. "Effect of the number of blades on undershot waterwheel performance for straight blades." In *IOP Conference Series: Earth and Environmental Science*, vol. 431, no. 1, p. 012024. IOP Publishing, 2020. https://doi.org/10.1088/1755-1315/431/1/012024
[15] Siswantara, Ahmad Indra, Budiarso Budiarso, Aji Putro Prakoso, Gun Gun R. Gunadi, Warjito Warjito, and Dendy Adanta. "Assessment of turbulence model for cross-flow pico hydro turbine numerical simulation." *CFD Letters* 10, no. 2 (2018): 38-48.
[16] Alfarawi, Suliman. "Evaluation of hydro-thermal shell-side performance in a shell-and-tube heat exchanger: CFD approach." *Journal of Advanced Research in Fluid Mechanics and Thermal Sciences* 66, no. 1 (2020): 104-119.
[17] Adanta, Dendy, Budiarso Budiarso, Warjito Warjito, and Ahmad Indra Siswantara. "Assessment of turbulence modelling for numerical simulations into pico hydro turbine." *Journal of Advanced Research in Fluid Mechanics and Thermal Sciences* 46, no. 1 (2018): 21-31.
[18] Yusuf, Siti Nurul Akmal, Yutaka Asako, Nor Azwadi Che Sidik, Saiful Bahri Mohamed, and Wan Mohd Arif Aziz Japar. "A short review on rans turbulence models." *CFD Letters* 12, no. 11 (2020): 83-96. https://doi.org/10.37934/cfdl.12.11.8396
[19] Khalil, Hesham, Khalid Saqr, Yehia Eldrainy, and Walid Abdelghaffar. "Aerodynamics of a trapped vortex combustor: A comparative assessment of RANS based CFD models." *Journal of Advanced Research in Fluid Mechanics and Thermal Sciences* 43, no. 1 (2018): 1-19.
[20] Rahman, Tariq Md Ridwanur, Waqar Asrar, and Sher Afghan Khan. "An Investigation of RANS Simulations for Swirl-Stabilized Isothermal Turbulent Flow in a Gas Turbine Burner." *CFD Letters* 11, no. 9 (2019): 14-31.
[21] Hakim, Muhammad Luqman, Bagus Nugroho, Rey Cheng Chin, Teguh Putranto, I. Ketut Suastika, and I. Ketut Aria Pria Utama. "Drag penalty causing from the roughness of recently cleaned and painted ship hull using RANS CFD." *CFD Letters* 12, no. 3 (2020): 78-88. https://doi.org/10.37934/cfdl.12.3.7888
[22] ANSYS Fluent. "Release 15.0, Theory Guide." *ANSYS Inc, Canonsburg* (2013).
[23] Alfarawi, Suliman, Azeldin El-sawi, and Hossin Omar. "Exploring Discontinuous Meshing for CFD Modelling of Counter Flow Heat Exchanger." *Journal of Advanced Research in Numerical Heat Transfer* 5, no. 1 (2021): 26-34.
[24] Roache, Patrick J. *Verification and validation in computational science and engineering. Vol. 895*. Albuquerque, NM: Hermosa, 1998.
[25] Young, Donald F., Bruce R. Munson, Theodore H. Okiishi, and Wade W. Huebsch. *Fundamentals of Fluid Mechanics*. John Wiley & Sons. Inc., USA (2006).